JCTC Journal of Chemical Theory and Computation

Article

pubs.acs.org/JCTC

How Many Ligands Can Be Bound by Magnesium–Porphyrin? A Symmetry-Adapted Perturbation Theory Study

Dorota Rutkowska-Zbik*,[†] and Tatiana Korona*,[‡]

[†]Jerzy Haber Institute of Catalysis and Surface Chemistry, Polish Academy of Sciences, ul. Niezapominajek 8, 30-239 Cracow, Poland

[‡]Faculty of Chemistry, University of Warsaw, ul. Pasteura 1, 02-093 Warsaw, Poland

Supporting Information

ABSTRACT: The stability of complexes of magnesium–porphyrin with one or two identical ligands from the set water, pyridine, imidazole, acetate, acetonitrile, dimethyl sulfoxide (DMSO), ethyl acetate, or acetylacetone was examined using symmetry-adapted perturbation theory (SAPT) for minimum geometries obtained by density-functional theory (DFT). The nonadditive contributions to the interaction energy of the porphyrin ring with two ligands were also included and found to be very small in almost all cases. The stability of the complexes under standard conditions is predicted on the basis of the free Gibbs energy. The analysis of individual components of the SAPT interaction energy allows us to explain why the complexation of the second ligand is not energetically preferred in some cases.

1. INTRODUCTION

Porphyrins constitute a family of macrocyclic ligands composed of four pyrrole units connected via methine groups in α positions. They may accommodate metal ions, usually on their +2 or +3 oxidation state, inside their cavity. Such a tetradentate coordination often does not satisfy the coordination number of central metal; therefore, metalloporhyrins are able to bind additional ligands in axial positions.

Magnesium porphyrins (Mg–Por) attract special attention as they serve as model compounds for chlorophylls or bacteriochlorophylls, the key components of the photosynthetic apparatus in plants, bacteria, and algae. Consequently, the main area of research in Mg–Por is focused on their photophysical properties, which may advance our understanding of light-harvesting processes and energy conversion during photosynthesis. Their interaction with the immediate surroundings, such as potential axial ligands, seems to be a less explored subject. This might be somewhat surprising, taking into account the importance of ligand-binding properties in the process of folding of photosynthetic proteins or the formation of pairs and larger supramolecular aggregates composed of (bacterio)-chlorophylls. Moreover, *in vitro* studies of Mg–Por and chlorophylls show that Mg–Por interactions with solvent molecules may influence their physicochemical properties (e.g., redox potentials, peak positions in UV–vis spectra[1,2]) and reactivity (e.g., in metalation, transmetalation[3,4]). It is also found that, although in the majority of magnesium compounds the Mg^{2+} ion is bound preferentially to six ligands, in the case of porphyrin and chlorophyll species *in vivo*, the Mg^{2+} coordination number is lower and rarely exceeds five.[5,6] Six-coordination of magnesium porphyrins was detected *in vitro*, mostly for non-native ligands such as, e.g., pyridine or tetrahydrofuran.[7,8] The existence of six-coordinated complexes with some amino acids was also predicted from the analysis of circular dichroism and optical rotatory dispersion spectra.[9,10] While the five-coordinate X-ray structure of magnesium tetraphenylporphyrin with one water molecule as an axial ligand has been resolved,[11,12] to our knowledge no structure with two axial water ligands has been reported so far. A fraction of six-coordinated bacteriochlorophylls is also found in the light harvesting I complex (LH1) of photosynthetic antennae.[13]

1.1. Existing Calculations for Complexes of Mg–Por.

The existing theoretical calculations of magnesium porphyrins concentrate mainly on the description of their electronic structure and spectroscopic properties, which is due to the fact that they may serve as model compounds for (bacterio)-chlorophylls. The electronic structure, energetics of frontier orbitals, and character of low-lying excited states were already examined at semiempirical [Parametrized Model 3 (PM3), Zerner's Intermediate Neglect of Differential Overlap parametrized for spectroscopic properties (ZINDO/S)], ab initio [Configuration Interaction Singles (CIS), Configuration Interaction Singles with Doubles correction (CIS(D)), Algebraic Diagrammatic Construction through second order (ADC(2)), Partially Renormalized ADC(2) (PR-ADC(2))][14,15], and DFT [mostly with the Becke, three-parameter, Lee–Yang–Parr (B3LYP) functional] levels.[16,17] Moreover, a number of theoretical studies on more complete chlorophyll/bacteriochlorophyll models, either represented by a simple chlorin or bacteriochlorin ligand or including all natural substituents, are known (see refs 17–20 and a recent review in ref 1).

The problem of the axial ligation of magnesium porphyrin is less studied, in spite of its importance for the Mg–Por chemistry and (in the case of (bacterio)chlorophylls) folding of photosynthetic proteins and the still incomplete understanding of the lower magnesium coordination number within these complexes. Among a few works which deal with this issue, we can name, e.g., the contribution of Elkin et al.,[21] where the thermodynamic stability of five-coordinate complexes of Mg–Por or chlorin with imidazole was predicted on the DFT-

Received: April 6, 2012
Published: July 5, 2012

(B3LYP) level.[21] Five- and six-coordinate complexes of Mg−Por with water and pyridine were examined at the MP2, DFT, and DFT+D (also with the B3LYP functional) levels by Fredj et al.[22] Whereas the binding of two water molecules is not exergonic, the thermodynamically stable complex with two pyridine ligands is found in ref 22. The authors attribute the difference of the complexation behavior of water and pyridine ligands to the dispersion interaction. However, the inclusion of dispersion through the Grimme (+D) correction[23−25] is far from being satisfactory, given a predicted crucial role of this effect. Further, Fredj et al. employed the B3LYP+D methodology to study the binding of water, pyridine, DMSO, acetone, acetonitrile, and tetrahydrofuran (THF) to chlorophyll.[26] According to their results, all studied solvents are able to form stable five-coordinate systems. The binding of the second ligand is found to be exothermic for all investigated ligands but, owing to the entropic contribution, is endoenergonic only for pyridine and THF.

Heimdal et al.[27] studied ligand-binding properties of magnesium chlorin and bacteriochlorin enlarged by the cyclopentanone ring, which serve as models of chlorophyll and bacteriochlorophyll, respectively, using DFT with the Becke−Perdew (BP) functional. Their results suggest that the binding of the sixth bioligand to the studied magnesium chelates would result in no gain of energy and, therefore, is thermodynamically unprivileged.

Oba and Tamiaki[5] employed molecular dynamics to assess the performance in the ligand binding of two faces of (bacterio)chlorophylls, which are nonequivalent because of the presence of various macrocycle substituents. They found that the position of the fifth ligand is determined by the existence of substituents which are able to form hydrogen bonds with the axial ligand.

The polarity of the environment determines the water binding by Mg−Por, chlorin, and bacteriochlorin, as was claimed on the basis of DFT(BP) studies.[28] This finding is in agreement with the observed influence of the environment's dielectric constant on structures of magnesium complexes with acidic and neutral ligands present in numerous proteins.[29] It was also proposed that on the basis of the experimental results, the lack of six-coordination in chlorophylls may be due to the drastic change of the hardness of the metal cation.[30]

Therefore, the aim of the present work is to explore the possibility of forming five- and six-coordinate magnesium porphyrin complexes with selected ligands (water, pyridine, imidazole, acetate, acetonitrile, DMSO, ethyl acetate, acetylacetone) and to define factors determining their stability with the help of the interaction energy decomposition in terms of symmetry-adapted perturbation theory (SAPT). Contrary to DFT+D, the SAPT approach treats the dispersion energy on an *ab initio* level, which will allow us to make more reliable conclusions about the stability of Mg−Por complexes. The selection of ligands for the present study is based on their popularity as solvents in experimental studies of chlorophylls.[31] X-ray structures of Mg−Por complexes with pyridine and water are available,[7,11,12] allowing for a comparison of structural parameters. In addition to this set, two anionic ligands were selected: acetate and acetylacetone. The first of these two ligands is known to facilitate the central-metal exchange in tetrapyrroles by its coordination to magnesium,[3] and the second anionic ligand (acetylacetone) might play a similar role.

1.2. Method. The stability of the complex *AB* is mostly determined by the interaction energy, defined as a difference between the electronic energies of the complex *AB* and the so-called monomers *A* and *B*, where the geometries of *A* and *B* remain unchanged in *AB*,

$$E_{\mathrm{int}}(AB) = E(AB) - E(A) - E(B) \tag{1}$$

If this energy is calculated for the minimum geometry, then thermal corrections for the free energy $\Delta g(T)$ can be added to judge the thermodynamic stability of the complex,

$$\Delta G(T) = E_{\mathrm{int}} + \Delta g(T) \tag{2}$$

$\Delta g(T)$ comprises the zero-point vibrational (ZPVE) and thermal vibrational ($\Delta u(T)$) energy corrections, rotational and translational corrections, and entropic contributions,

$$\Delta g(T) = \Delta E_{\mathrm{ZPVE}} + \Delta u(T) + \Delta(E_{\mathrm{rot}} + E_{\mathrm{transl}} + pv) - T\Delta S \tag{3}$$

and in the studied cases (only nonlinear molecules are studied)

$$\Delta(E_{\mathrm{rot}} + E_{\mathrm{transl}} + pv) = -4RT \tag{4}$$

Although it is in principle possible to obtain the minimum of the potential energy surface (PES) defined by eq 1, it is rarely done in practice, especially for larger molecules. If the stability of the complex is required, one usually minimizes separately the geometries of *AB*, *A*, and *B* and obtains the ZPVE and entropic contributions for the complex as a difference between these quantities for *AB* and monomers. If the same route is adopted for the electronic contributions, then the obtained number cannot be called the interaction energy any more, as the monomers have different geometries in *AB* and as separate molecules. The resulting quantity then contains the interaction energy and the so-called geometry-relaxation term. It should be emphasized that eq 1 defines the whole intermolecular PES, while the former energy is a single number defined just for the minimum geometry.

The interaction energy can be calculated either by the supermolecular method, i.e., directly from eq 1 with the exact energies replaced by approximate ones, or by the perturbation method, i.e., where this energy is obtained as a sum of some correction terms. Studies of stability of complexes with porphyrin performed so far emphasize the fact that a significant part of this energy may result from the dispersion interaction.[22] It is therefore important to include the dispersion energy as accurately as possible. The choice of supermolecular methods which account for dispersion and which can be applied to complexes of this size is however quite limited. One can use the Møller−Plesset method to the second order (MP2) or parametrized methods like spin-component-scaled MP2 (SCS-MP2).[32] It is however known that the MP2 method gives interaction energies which are often too low,[33] and although SCS-MP2 frequently corrects for this overbinding, it may show a mixed performance in some cases.[34] The DFT method is not expected to provide reasonable interaction energies because of the short-range character of the currently used DFT functionals, which makes it difficult to correctly describe the long-range correlation effects, like dispersion. On the other hand, the DFT+D method[23,24] can be exploited for these systems,[22] but final results will then depend on the quality of the parametrization: a feature which we prefer to avoid in any study aiming at high accuracy. A natural candidate for calculations involving noncovalently bonded species is symmetry-adapted perturbation theory (see refs 35−37 and references therein), where physically meaningful components,

like electrostatics, induction, dispersion, and their exchange counterparts, are calculated separately. If monomers in SAPT are described by DFT, the SAPT method starts to be competitive with MP2 as far as computational resources are concerned, providing at the same price the interaction energy which is known to be at the same level as Coupled Cluster Singles and Doubles with perturbative Triples (CCSD(T)) supermolecular energies[38,39] or benchmark SAPT(CCSD) energies.[40−46] It should also be added that the nonexpanded operator for the intermolecular interactions is used in SAPT, so the energy corrections are not affected by the well-known problems related to the divergence of the multipole expansion. It is important to notice that, contrary to the supermolecular case, the DFT method in SAPT(DFT) is only used to describe the (short-range) electron *intra*monomer correlation, which is well accounted for, while a difficult (long-range) *inter*monomer electron correlation, i.e., the dispersion interaction, is included through the SAPT method. The SAPT(DFT) method developed by Misquitta et al.[47−49] (see also ref 50) and independently by Jansen and Heßelmann[51−55] in the past 10 years has already gained great popularity, especially after the density-fitting (DF)[38,39,56−58] method has been employed to calculate the two-electron repulsion integrals (this method is also known as the resolution-of-identity (RI) method[59,60]). The SAPT(DFT) method with DF[38,39] can be used for van der Waals molecules as large as dimers of cyclotrimethylene trinitramine[61] or for endohedral complexes of fullerenes.[62]

In SAPT, the total Hamiltonian H of a dimer AB is divided into the unperturbed part H_0, being the sum of monomers' Hamiltonians H_A and H_B, and a perturbation V, which describes the electrostatic interaction between monomers. The SAPT interaction energy up to the second order in V is defined as a sum of three Rayleigh−Schrödinger corrections—first-order electrostatic ($E^{(1)}_{\mathrm{elst}}$), second-order induction ($E^{(2)}_{\mathrm{ind}}$), and second-order dispersion ($E^{(2)}_{\mathrm{disp}}$) energies—and their exchange counterparts, accounting for electron tunneling effects between monomers—first-order exchange ($E^{(1)}_{\mathrm{exch}}$), second-order exchange-induction ($E^{(2)}_{\mathrm{exch-ind}}$), and second-order exchange-dispersion ($E^{(2)}_{\mathrm{exch-disp}}$) energies. To this energy usually the so-called δE_{HF} correction[63,64] is added, which approximately accounts for the third and higher order induction and exchange-induction energies on the level of Hartree−Fock (HF) theory. The SAPT(DFT) approach has been shown recently[65] to provide good agreement with the hybrid "coupled" MP2 (MP2C) method[66,67] applied to complexes of rare gas atoms with the C_{60} fullerene. In the MP2C method, the supermolecular MP2 energy is corrected for a dispersion by replacing the uncoupled HF (UCHF) dispersion (known to be present in MP2 if the separation of the supermolecular MP2 energies is performed[68,69]) with the coupled Kohn−Sham (CKS) one.

The trimer interaction energy, defined as

$$E_{\mathrm{int}} = E(ABC) - E(A) - E(B) - E(C) \tag{5}$$

can be divided into the pairwise and nonadditive contributions, denoted as $E_{\mathrm{int}}[2,3]$ and $E_{\mathrm{int}}[3,3]$, respectively

$$E_{\mathrm{int}}[2,\,3] = E_{\mathrm{int}}(AB) + E_{\mathrm{int}}(BC) + E_{\mathrm{int}}(CA)$$

$$E_{\mathrm{int}}[3,\,3] = E(ABC) - E_{\mathrm{int}}[2,\,3] \tag{6}$$

The first part consists of the sum of three interaction energies of dimers and is obtained by invoking the SAPT(DFT) method three times. The second part can also be in principle obtained on a pure SAPT level, as shown in ref 61, but since many complicated components should be accounted for in this case, we adopted a more pragmatic MP2+SDFT approach, also presented in the same reference. The MP2+SDFT method relies on the observation that most nonadditive SAPT energy contributions are approximately included within the supermolecular MP2 energy (for the analogous reasons as given in refs 68 and 69), and the only missing term on the nonadditive MP2 level is the third-order dispersion energy [it appears in the supermolecular approach at the Møller−Plesset method to the third order (MP3) level]. Therefore, the nonadditive interaction energy is calculated as

$$E_{\mathrm{int}}[3,\,3] = E^{\mathrm{MP2}}_{\mathrm{int}}[3,\,3] + E^{(3)}_{\mathrm{disp}}(\mathrm{CKS})[3,\,3] \tag{7}$$

In summary, the total trimer interaction energy is calculated by the hybrid approach, where the largest part of the energy (the pairwise contributions and the nonadditive part of the third-order dispersion energy) is calculated with SAPT(DFT), and the remaining nonadditive part is obtained with the supermolecular MP2 approach.

Total and nonadditive supermolecular interaction energies are also calculated for the MP2, SCS-MP2, and HF methods, where the Boys−Bernardi counterpoise recipe[70] has been utilized to avoid the basis-set superposition error (BSSE).

2. COMPUTATIONAL DETAILS

Geometries of the complexes were optimized at the DFT level with the Becke-Perdew (BP) functional[71−75] as implemented in the TURBOMOLE v 6.3 suite of codes,[76,77] with the RI method used to accelerate the computations.[78] The harmonic frequencies analysis was performed to confirm that the obtained stationary points are indeed minima. The def1-TZVP basis set was used for atomic orbitals,[79] while the corresponding auxiliary basis sets[80] were utilized for RI. This basis is somewhat smaller than a corresponding newer basis (def2-TZVP) from the *X*ZVP family, which is important in view of the computational cost of the DFT geometry optimization and frequency analysis. Geometry optimization employing a smaller basis set than the final energy computation is a common procedure in DFT applications (see, e.g., ref [81]), but in order to check the influence of the basis set size on the geometry of the studied complexes, the Mg−Por system with two pyridine ligands has been optimized also with def2-TZVP. The difference in Mg−Por−pyridine distances obtained with def1-TZVP and def2-TZVP is only 0.001 Å. It can then be concluded that the application of a smaller basis set has a negligible effect on geometries. Further, a single optimization for the complex of Mg−Por with two pyridine molecules has been performed with the usage of the "+D3" correction of Grimme et al.[25] It turned out that differences in optimized geometry parameters and SAPT interaction energies obtained for both geometries were small in this case: total interaction energies are equal to −45.60 and −45.66 mhartree for geometries optimized without and with the "+D3" correction, respectively. Since analytical harmonic frequencies are not available for the DFT+D method, we decided to use a standard DFT optimization for all other complexes. The harmonic frequencies from the DFT optimization were utilized later in the calculation of the free Gibbs energy for the complexation reaction. The error associated with this choice stems from the harmonic approximation itself, the usage of the DFT method, and the incomplete orbital basis set. Since DFT harmonic

frequencies are used routinely in many applications, many investigations have been performed to access their accuracy. A good estimate of an average error made when these frequencies are utilized is given by scaling factors for frequencies, proposed and widely used as a practical remedy for the known deficiencies of the DFT (or other method) frequencies (see, e.g., ref 82). These factors are usually on the order of 0.95 and simultaneously take into account the harmonic approximation and the DFT errors. Additionally, harmonic and anharmonic (vibrational spectra calculated from the same PES) allow one to access the quality of the harmonic approximation, which is usually also of about 5% (see, e.g., ref 83). We can therefore expect errors of this order of magnitude for the frequency-dependent terms.

All single-point calculations, like SAPT(DFT), MP2, and SCS-MP2, were performed with the MOLPRO suite of codes[84] at the BP-optimized geometries without further geometry changes. The PBE functional[85,86] was used in SAPT with the asymptotic correction of Grüning et al.[87] The ionization potentials needed for the calculation of the asymptotic corrections have been obtained from ref 88 for ligands and as a difference of the unrestricted Kohn–Sham (KS) energy for the cation and the restricted KS energy for the neutral molecule for Mg–Por. The def2-TZVP basis[89] has been used with the TZVP/MP2FIT[90] and cc-pVTZ/JKFIT[91] auxiliary bases. For three cases, SAPT calculations with a larger def2-QZVP basis[79] have been performed to check the saturation of the SAPT components with the basis set. Core electrons (1s for C, N, O, and Mg) have been frozen in all correlated calculations.

For several complexes, selected cuts through the PES have been additionally performed. For the case of the Mg–Por complexes with water and pyridine, the Mg–Por bent structure from the BP equilibrium geometry has been frozen, and the ligand was shifted on the line perpendicular to Mg–Por. A similar procedure was used also for several trimers; i.e., one ligand has been moved starting from the minimum trimer geometry, while the second ligand and the Mg–Por molecule were kept frozen. In this way, a dissociation process of one ligand can be simulated to a some extent. Finally, for Mg–Por···(water)$_2$ and Mg–Por···(pyridine)$_2$, the ligands were also shifted symmetrically along the Mg–Por axis, allowing us to investigate a simultaneous dissociation of the trimer into the monomers.

3. RESULTS AND DISCUSSION

The most important geometry parameters found for dimers and trimers from the BP optimization are listed in Table 1 and shown in Figures 1 and 2. Both studied anionic ligands are able to coordinate to magnesium ions as mono- or bidentate ligands, forming either one or two bonds, respectively. Therefore, for systems containing acetate and acetylacetone, two starting structures were considered: with mono- and bidentate modes of coordination. In studied dimers, the acetate molecule prefers the monodentate coordination, contrary to acetylacetone, where the bidentate one is energetically favored. In trimers, both acetate and acetylacetone are monodentate, in agreement with literature data.[29,92] A stable structure of Mg–Por (acetate (2))$_2$ is found, but the obtained Mg–Por–ligand bond lengths (>3.00 Å) are too long to be considered as being in the range of a typical chemical bonding. Further, the optimal structure of Mg–Por (acetylacetone (2))$_2$ has not been found: geometry optimization of the structure led always to Mg–Por (acetylacetone (1))$_2$ for all tried starting geometries. A scan of the BP PES with simultaneous changes in Mg–Por–acetylacetone bond lengths shows no minima corresponding to the stable Mg–Por (acetylacetone (2))$_2$ (see the Supporting Information).

Table 1. BP-Optimized Mg–Por···L Bond Lengths in the Studied Dimers (Second Column) and Trimers (Third Column) and Mg out-of-Plane Displacements in Respective Dimers[a]

ligand	Mg–Por···L	Mg–Por···L$_2$	Mg out-of-plane
water	2.205	2.298; 2.298	0.26
pyridine	2.250	2.439; 2.439	0.32
DMSO	2.116	2.259; 2.260	0.36
acetonitrile	2.261	2.392; 2.396	0.30
ethyl acetate	2.153	2.322; 2.327	0.33
imidazole	2.214	2.356; 2.356	0.37
acetate (1)	1.997	2.184; 2.185	0.57
acetate (2)	2.257; 2.303	3.063; 3.071; 3.063; 3.071	0.60
acetylacetone (1)	1.991	2.266; 2.268	0.54
acetylacetone (2)	2.191; 2.191		0.75

[a]Bond lengths are calculated between the magnesium ion and the donor atom of the ligand (see Figures 1 and 2). In the case of the chelating ligands (acetate (2) and acetylacetone (2)), distances to both donor atoms are listed. Mg out-of-plane displacement is calculated as a distance between Mg and a plane which spans over nitrogen atoms from the porphyrin macrocycle. Distances are in Ångstroms.

Overall, the computed geometries are in agreement with experimental observations. In all dimers, the porphyrin ring is bent with the Mg ion considerably pulled out of plane toward the incoming ligand. Such a deformation was already found in the structures of five-coordinate complexes of Mg–Por.[11,12] The effect is the least pronounced in Mg–Por···water, where calculated Mg displacement is by 0.01 Å smaller than that found in the X-ray crystal structure of aqua-magnesium porphyrin.[11] The geometry is the most affected in complexes with both anionic ligands (acetate and acetylacetone), which is in agreement with the proposed strong deformation of Mg–Por in the presence of acetate in solution.[3] In general, Mg–Por–ligand bonds are shorter in dimers than in trimers. The calculated Mg–Por···water bond length is longer than the respective values found in the X-ray structures of five-coordinate magnesium porphyrins with water,[11,12] where Mg···water distances are equal to 2.099 Å and 2.012 Å, respectively. Such a short bond between Mg and water was ascribed there to the strong interaction of the coordinated water with cosolvent molecules used for crystallization. Mg–Por···pyridine bond distances in the investigated trimer are by 0.05 Å longer than in the respective crystal structure.[7]

Table 2 presents the SAPT components and the total interaction energies for SAPT(DFT), MP2, SCS-MP2, and HF theories for the Mg–Por–ligand complex. The BP optimized geometry corresponds then to the bent Mg–Por molecule. In Table 3, the same data are presented for three dimer pairs in the Mg–Por···L$_2$ trimer. In this case, the BP optimized trimer geometry has been used, where each time one molecule was removed. Since SAPT is by definition BSSE-free, no basis on ghost atoms of the third monomer was used for pair-interaction energies (i.e., a dimer-centered basis set was used to obtain pairwise interaction energies also for the trimer case). The resulting dimer interaction energies are used as the additive part of the total trimer interaction energy. In the trimer, the Mg–

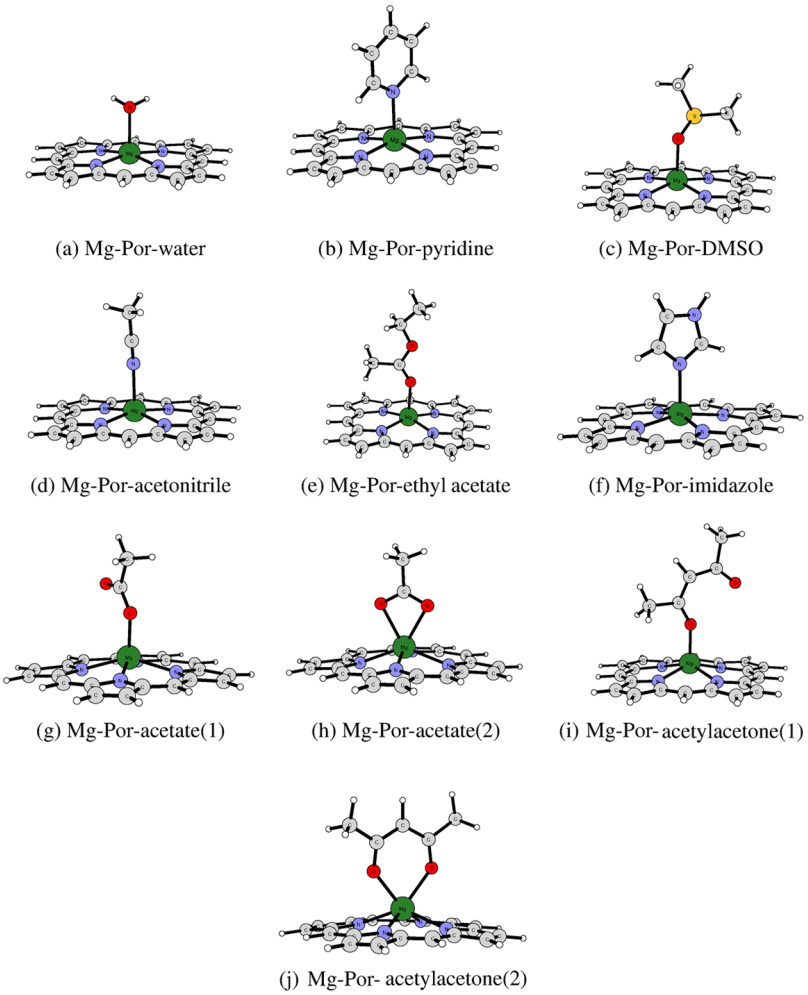

Figure 1. Structures of the investigated dimers.

Por molecule is planar, which results in a substantial decrease of the absolute values of the electrostatic and induction energies of the Mg−Por···L complexes. This effect can be explained by the fact that the bent Mg−Por complex possesses a sizable dipole moment (of value of about 2.5 D from the BP calculation), which results in a stronger electrostatic attraction of the ligand in the first order of perturbation theory and in a larger induction effect in the direction Mg−Por to ligand. On the other hand, in the planar Mg−Por, a dipole moment is absent, which makes the electrostatics and induction much less significant.

Additionally, Figures 3 and 4 for water and pyridine ligands show the dependence of the SAPT contributions on the distance between the center of the Mg−Por molecule and the oxygen atom (for water) or the nitrogen atom (for pyridine). In the bent Mg−Por complex with water, there is a sizable first-order contribution which can be explained by a dipole moment of the bent Mg−Por. Similarly, the sum of the second-order induction and exchange-induction energies gives substantial contributions in this case, while the dispersion plus exchange-dispersion gives similar values for bent and planar cases. It should be noted that in the case of nonpolar monomers, the induction energy at the van der Waals minimum region may also be quite large, but it is almost completely quenched by its exchange counterpart. The netto induction effect in the intermolecular energy appears only if at least one of the monomers is polar. The decisive factor for a larger stability of the complexes with pyridine is the dispersion interaction. Our results therefore confirm the findings of Fredj et al.,[22] which were obtained with the more approximate DFT+D method.

In Tables 2 and 3 also the supermolecular energies are presented for the MP2, SCS-MP2, and HF methods. As usual for complexes with conjugated bonds,[33,65] the MP2 approach predicts much too low interaction energies. SCS-MP2 corrects this overbinding to some extent, but still differences up to 20% can be detected with respect to SAPT(DFT). Interestingly, the closest agreement with SAPT(DFT) in Table 2 is given by the HF interaction energies. However, this good agreement is in this case a lucky coincidence, since HF does not contain the dispersion energy, which is an important part of the interaction energy for SAPT(DFT). This fact becomes evident when Table 3 is examined. Here, the HF energies for the Mg−Por···L dimers (from the Mg−Por···L_2 trimer) can be even 2 times too small in the absolute value (see the complex with pyridine). On the other hand, it can be clearly seen that for the interaction of two ligands, which are far apart from each other, the dominating contribution is the electrostatic energy. This should be evident as the electrostatic component decreased with the inverse cubic power of R (a distance between monomers) for dipoles or with the inverse power of R (for anions acetate and acetylacetone). This contribution is always repulsive, since the optimal placement of the ligands is governed by their binding

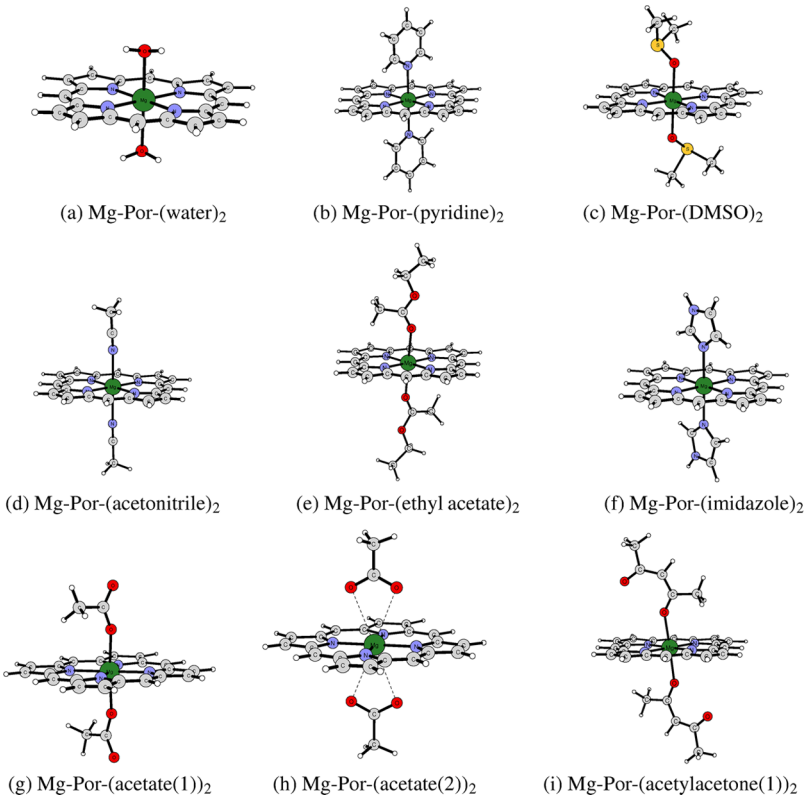

Figure 2. Structures of the investigated trimers.

Table 2. Components of the SAPT Interaction Energy and Total Energies Calculated with Various Methods for Complexes of the Bent Mg−Por with a Ligand Calculated at BP Minimum Geometries[a]

ligand	$E^{(1)}_{elst}$	$E^{(1)}_{exch}$	$E^{(2)}_{ind}$	$E^{(2)}_{exch-ind}$	$E^{(2)}_{disp}$	$E^{(2)}_{exch-disp}$	δE_{HF}	$E_{SAPT}(2)$	E_{SAPT}	E_{MP2}	$E_{SCS-MP2}$	E_{HF}
water	−40.74	39.60	−51.76	42.50	−12.74	3.18	−0.94	−19.96	−20.90	−25.68	−23.96	−20.25
pyridine	−54.90	54.96	−83.56	68.83	−24.03	5.06	−0.56	−33.64	−34.20	−43.93	−39.77	−26.73
imidazole	−57.82	54.85	−88.28	71.57	−21.84	4.83	0.04	−36.68	−36.64	−45.95	−42.55	−31.99
acetate (1)	−94.82	71.72	−153.89	110.75	−21.42	6.49	−0.87	−81.18	−82.05	−89.96	−88.05	−82.69
acetate (2)	−99.28	79.19	−156.30	111.05	−28.06	8.89	−6.34	−84.51	−90.85	−101.15	−97.96	−87.39
acetonitrile	−35.01	36.24	−48.26	37.07	−13.87	2.90	−1.28	−20.91	−22.19	−27.76	−25.47	−17.96
DMSO	−50.83	51.51	−77.98	62.50	−22.41	4.76	−2.28	−32.45	−34.73	−44.89	−41.63	−34.09
ethyl acetate	−39.70	41.28	−56.06	44.00	−18.64	3.71	−2.70	−25.41	−28.11	−34.36	−31.43	−25.21
acetylacetone (2)	−105.28	94.13	−141.84	94.81	−36.92	10.34	−11.25	−84.77	−96.02	−110.16	−105.81	−95.22
acetylacetone (1)	−79.05	64.85	−122.36	86.96	−23.62	6.13	−3.20	−67.10	−70.30	−79.68	−77.19	−71.02

[a]The number in parentheses after the molecule name denotes the number of bonds the ligand creates with the Mg atom. $E_{SAPT}(2)$ denotes the sum of six SAPT components, while E_{SAPT} denotes the total recommended SAPT energy, where also the δE_{HF} has been added. In the last three columns, the supermolecular energies are presented. Energies are in millihartrees.

to Mg−Por, so adding a second ligand will always cause an electrostatic repulsion of two ligands to be switched on, causing a first-order destabilization effect on the trimer. The only force which can bind two ligands are the second-order effects, but for polar ligands they decrease with R much quicker than the $E^{(1)}_{elst}$ and give negligible contributions in all cases. Therefore, the repulsive electrostatic components from the L···L interaction should be quenched by some attractive components of the Mg−Por···L interaction energy. For two anionic ligands, it was not possible, which is indicated by the positive additive part of the interaction trimer energy, see Table 4. In this table, the total interaction energies of the trimers and the nonadditive parts of the energy from MP2+SDFT are presented. As can be seen, the nonadditive contributions are not important, with the exception of acetylacetone, since they give about 1% of the total interaction energy. For the acetylacetone case, one can see from Table 3 that two negative SAPT energies for Mg−Por···acetylacetone cancel to a large extent with the large positive L···L energy, so the nonadditive part in this case is only about 7% of the latter energy.

The zero-point vibrational energies and temperature-dependent terms are obtained as a byproduct of the BP minimalization. The resulting free Gibbs energies, with the electronic parts taken from Tables 2 and 4, as well as their consecutive components are presented in Table 5. The changes of Gibbs free energies accompanying studied complex formation reveal that all dimers exist at room temperature. ΔG's of formation of Mg−Por···water and Mg−Por···acetonitrile are comparable and, at the same time, the smallest in the investigated set of compounds. Binding of the anionic ligands is considerably

Table 3. Components of the SAPT Interaction Energy and Total Energies Calculated with Various Methods for Three Pairs in the Trimer[a]

ligand	$E^{(1)}_{elst}$	$E^{(1)}_{exch}$	$E^{(2)}_{ind}$	$E^{(2)}_{exch-ind}$	$E^{(2)}_{disp}$	$E^{(2)}_{exch-disp}$	δE_{HF}	$E_{SAPT}(2)$	E_{SAPT}	E_{MP2}	$E_{SCS-MP2}$	E_{HF}
water	−36.12	40.57	−45.13	37.97	−14.29	3.55	−1.29	−13.45	−14.74	−19.12	−17.05	−11.73
	(−35.75)	(40.54)	(−45.49)	(38.13)	(−16.79)	(3.98)		(−15.38)				
	−36.12	40.57	−45.19	38.02	−14.30	3.55	−1.29	−13.46	−14.75	−19.12	−17.05	−11.73
	1.42	0.01	−0.02	0.00	−0.06	0.00	0.00	1.35	1.35	1.45	1.45	1.54
pyridine	−39.67	47.69	−53.04	44.92	−26.27	5.26	−1.95	−21.11	−23.06	−32.97	−27.80	−10.85
	−39.67	47.69	−53.04	44.92	−26.28	5.26	−1.95	−21.11	−23.06	−32.97	−27.80	−10.85
	1.69	0.03	−0.10	0.01	−0.36	0.01	0.00	1.28	1.28	1.37	1.48	1.83
imidazole	−44.18	51.69	−63.88	53.31	−25.17	5.35	−1.27	−22.88	−24.15	−34.02	−29.45	−14.38
	−44.11	51.55	−63.35	52.79	−25.07	5.31	−1.26	−22.88	−24.14	−34.02	−29.45	−14.39
	3.12	0.05	−0.19	0.01	−0.35	0.01	0.01	2.66	2.67	2.92	3.03	3.41
acetate	−47.72	57.92	−89.30	62.02	−26.32	7.15	−3.29	−36.25	−39.55	−46.62	−42.92	−29.60
	−47.38	57.99	−88.99	61.67	−26.19	7.13	−3.31	−35.77	−39.09	−46.10	−42.43	−29.18
	87.34	0.04	−2.37	0.02	−0.28	0.01	0.10	84.76	84.86	85.41	85.68	87.49
acetonitrile	−25.61	32.93	−32.91	25.72	−14.78	2.99	−1.61	−11.66	−13.28	−18.73	−16.03	−6.38
	(−25.55)	(32.65)	(−33.32)	(26.00)	(−16.40)	(3.27)		(−13.35)				
	−25.88	33.16	−34.20	27.00	−14.77	3.01	−1.60	−11.69	−13.28	−18.84	−16.15	−6.56
	2.53	0.01	−0.11	0.00	−0.15	0.00	0.00	2.29	2.29	2.28	2.31	2.73
DMSO	−38.14	48.32	−57.33	47.53	−24.59	5.08	−2.75	−19.13	−21.88	−31.57	−27.32	−15.11
	−38.24	48.56	−56.88	47.05	−24.73	5.10	−2.81	−19.15	−21.97	−31.74	−27.45	−15.15
	2.82	0.02	−0.16	0.01	−0.27	0.00	0.01	2.42	2.43	2.65	2.82	3.92
ethyl acetate	−26.97	35.52	−33.78	26.86	−19.25	3.61	−2.72	−14.01	−16.73	−22.77	−19.29	−9.48
	(−26.93)	(35.30)	(−34.36)	(27.22)	(−21.52)	(3.98)		(−16.31)				
	−26.64	35.07	−21.96	14.85	−18.85	3.52	−2.80	−14.01	−16.81	−22.42	−19.02	−9.45
	1.87	0.01	−0.11	0.00	−0.20	0.00	0.00	1.56	1.57	1.49	1.55	2.26
acetylacetone	−38.19	50.31	−74.76	53.26	−26.74	6.40	−3.51	−29.70	−33.21	−41.07	−36.87	−22.44
	−37.59	49.85	−73.83	52.29	−26.61	6.35	−3.55	−29.54	−33.08	−40.78	−36.63	−22.33
	76.58	0.03	−2.71	0.01	−0.34	0.01	0.14	73.58	73.73	74.13	74.47	77.61

[a]For each molecule, the consecutive rows give the Mg−Por−first ligand, Mg−Por−second ligand, and first ligand−second ligand interaction energies. For water, acetonitrile, and ethyl acetate SAPT components for the first dimer obtained in the def2-QZVP basis are given in parentheses. Energies are in millihartrees.

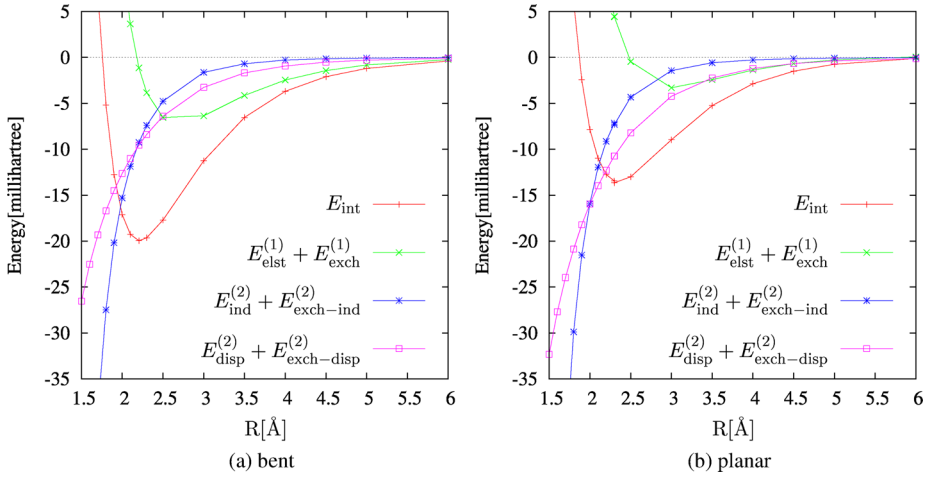

Figure 3. Interaction energy components for the bent and planar Mg−Por complexes with water.

more favorable for the Mg−Por−ligand system than binding of other neutral species, which according to Table 2 should be attributed to larger electrostatic and induction effects. Although the stability of all studied trimers with neutral ligands at 0 K is confirmed by changes of interaction energies ΔE_{int} (a small ZPVE contribution does not affect this conclusion), the introduction of thermal corrections indicates that most of them are not formed at room temperature, where only two trimers might exist: Mg−Por···(pyridine)$_2$ and Mg−Por···(imidazole)$_2$. Complexes with anionic ligands are not stable even at 0 K. The reason for this is, as already mentioned, the large long-range electrostatic repulsion of ligands, which cannot be fully quenched by the shorter-range Mg−Por···acetylacetone (or acetate) attractive SAPT energy components. For water, acetonitrile, and ethyl acetate ligands, the Gibbs energy is quite small, so it might be possible that the use of a more saturated basis set would make these energies negative at room temperature. Therefore, for these three ligands, we performed additional computations in a larger def2-QZVP basis. (The recalculation of all data with this basis would take 3−4 times

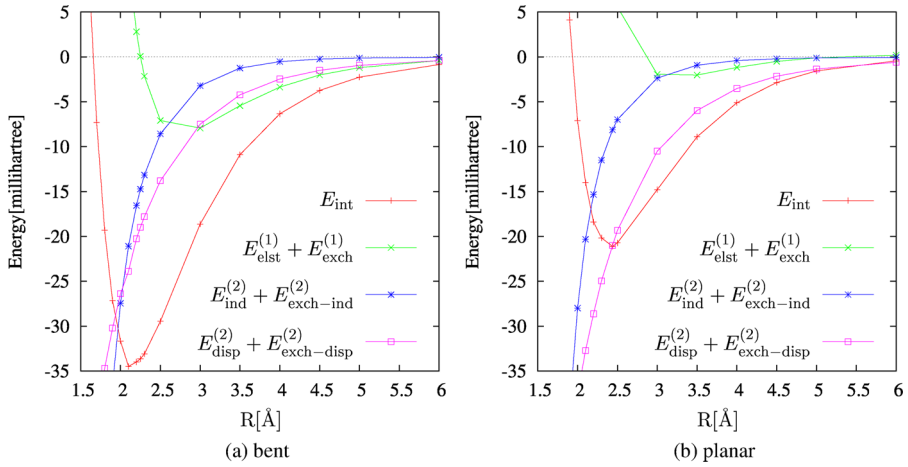

Figure 4. The interaction energy components for the bent and planar Mg−Por complexes with pyridine.

Table 4. Nonadditive Components of the SAPT Interaction Energy and Total Energies of Trimers Calculated with Various Methods[a]

ligand	$E^{(3)}_{disp}$[3,3](CKS)	E_{MP2}[3,3]	E_{SAPT}[2,3]	$E_{hybridSAPT}$	E_{MP2}	$E_{SCS-MP2}$	E_{HF}
water	−0.10	−0.57	−28.14	−28.81	−37.70	−33.53	−22.68
pyridine	−0.29	−0.46	−44.84	−45.60	−65.28	−54.80	−20.34
imidazole	−0.31	−0.94	−45.62	−46.87	−66.26	−57.00	−26.35
acetate	−0.39	0.10	6.23	5.93	−5.95	1.62	28.46
acetonitrile	−0.14	−0.55	−24.27	−24.95	−35.93	−30.50	−10.75
DMSO	−0.28	−0.81	−41.42	−42.51	−61.65	−52.92	−27.50
ethyl acetate	−0.17	−0.25	−31.97	−32.38	−44.10	−37.11	−17.03
acetylacetone	−0.38	4.82	7.44	11.88	−1.91	6.85	37.56

[a]Energies are in millihartrees.

longer than with the current basis, which already took 1−2 days per point.) As expected, the improvement of the basis has an effect mostly on the $E^{(2)}_{disp}$ term, which is known for its sensitivity to basis quality. In total, the pairwise interaction energy for the Mg−Por···$(water)_2$ complex was lowered by 4.1 mhartree when going from def2-TZVP to def2-QZVP. The remaining unsaturation effect can be estimated by taking a formula for the complete-basis-set (CBS) limit of the correlation energy,[93−95]

$$E(\text{Basis}[X]) = E(\text{CBS}) + A/X^3 \quad (8)$$

where X is the basis "quantum number". Taking $X = 3$ and 4 for def2-TZVP and def2-QZVP,[96,97] respectively, one can estimate the remaining effect as −3 mhartree. This gives a total lowering of the pairwise interaction energy by 9 mhartree, which might suggest a slight thermodynamical stability of this complex at room temperature. However, with such a small number, more factors should be taken into account, like more accurate inclusion of the nonadditive energies and the fourth-order SAPT effects. In summary, it seems probable that the complex of Mg−Por with two waters will be stable for temperatures a bit lower than 298.15 K. For complexes with acetonitrile and ethyl acetate, the change of the pairwise interaction energy amounts to −3.3 and −4.7 mhartree, respectively, while the application of eq 8 gives the total CBS correction equal to −6 and −9 mhartree, in comparison to the def2-TZVP basis results. Therefore, in these two cases also a slight stabilization is predicted.

Our findings regarding the stability of studied systems are confirmed by the existence of X-ray structures of five-coordinate complexes with water and six-coordinate complexes with pyridine. Further, a coordination equilibrium of bacteriochlorophyll with pyridine is shifted toward hexacoordination.[31]

Finally, it should be noted that ZPVE accounts only for up to 16% of the thermal correction to the free energy, while the most significant contribution originates from the entropy correction.

It is also interesting to examine how the ligand complexation can affect the lowest electronic transitions of Mg−Por, which fall into the visible region. To this end, we performed the EOM-CCSD,[98] as implemented in MOLPRO,[99] of planar Mg−Por (to keep the highest possible spatial symmetry) with one or two water molecules with the cc-pVDZ basis.[100] To avoid a bias which would be caused by using different basis sets, the basis was placed also on the ghost water atoms, as it is usually done in counterpoise calculations. Although we are aware that the selected basis is not sufficient for quantitative predictions, it might be nonetheless useful to show general trends for the lowest states (it has been checked for the Mg−Por···$(water)_2$ case that the aug-cc-pVDZ basis causes a lowering of the excitation energy by 0.03 eV only). Because of huge time requirements for such calculations, only right-hand-side EOM vectors were obtained, and the oscillator strengths were calculated from formula 38 of ref 44, assuming (approximately) the equality of left and right transition moments. The presence of two water ligands lowers the symmetry to C_{2v}, which results in a slight splitting of the degenerate lowest 1^1E_u state of a noncomplexated Mg−Por. It can be observed that this splitting of the excitation energy is small for H_2O ligands (0.005 eV for one water and 0.02 eV for two waters). More importantly, a

Table 5. Interaction Energies and Thermodynamic Quantities of the Studied Complexation Processes (T = 298.15 K, p = 0.1 MPa)[a]

reaction	$\Delta G(T)$	E_{int}	ΔZPVE	$\Delta u(T)$	$T\Delta S$	$\Delta g(T)$
Mg−Por + water	−6.53	−20.90	2.56	3.56	12.03	14.37
Mg−Por +2 water	3.37	−28.81	4.97	6.97	27.80	32.18
Mg−Por (water) + water			2.41	3.41	15.77	17.81
Mg−Por + pyridine	−15.40	−34.20	1.49	4.54	16.54	18.80
Mg−Por +2 pyridine	−7.67	−45.60	2.02	9.21	34.25	37.93
Mg−Por (pyridine) + pyridine			0.53	4.67	17.71	19.13
Mg−Por + DMSO	−17.37	−34.73	0.99	4.62	15.53	17.36
Mg−Por +2 DMSO	−6.18	−42.51	1.49	9.31	33.08	36.33
Mg−Por (DMSO) + DMSO			0.50	4.69	17.56	18.96
Mg−Por + acetonitrile	−8.19	−22.19	0.84	4.66	12.27	14.00
Mg−Por +2 acetonitrile	0.69	−24.95	1.07	9.70	22.43	25.64
Mg−Por (acetonitrile) + acetonitrile			0.23	5.03	10.16	11.65
Mg−Por + ethyl acetate	−11.02	−28.11	0.91	4.77	15.18	17.09
Mg−Por +2 ethyl acetate	1.26	−32.38	1.03	9.98	30.19	33.64
Mg−Por (ethyl acetate) + ethyl acetate			0.11	5.21	15.01	16.55
Mg−Por + imidazole	−18.66	−36.64	1.33	4.55	15.88	17.98
Mg−Por +2 imidazole	−11.42	−46.87	1.56	9.52	31.92	35.45
Mg−Por (imidazole) + imidazole			0.23	4.97	16.05	17.47
Mg−Por + acetate (1)	−65.51	−82.05	0.27	4.72	15.34	16.54
Mg−Por + acetate (2)	−75.80	−90.85	−0.15	4.92	14.05	15.05
Mg−Por +2 acetate (1)	40.39	5.93	−0.65	9.35	33.31	34.46
Mg−Por +2 acetate (2)			−2.70	2.98	−67.87	43.22
Mg−Por (acetate (1)) + acetate (1)			−0.91	4.63	17.97	17.92
Mg−Por (acetate (2)) + acetate (1)			−0.50	4.43	19.26	19.41
Mg−Por (acetate (2)) + acetate (2)			−2.55	−1.94	−82.78	27.32
Mg−Por + acetylacetone (1)	−53.72	−70.30	0.57	4.80	14.99	16.58
Mg−Por + acetylacetone (2)	−76.95	−96.02	0.27	4.63	17.96	19.07
Mg−Por +2 acetylacetone (1)	42.67	11.88	−0.88	10.12	29.10	30.79
Mg−Por (acetylacetone (1)) + acetylacetone (1)			−1.45	5.32	14.12	14.21
Mg−Por (acetylacetone (2)) + acetylacetone (1)			−1.14	5.49	11.15	11.72

[a]Energies are in millihartrees.

slight redshift of excitation energies is observed when the water ligands are added to Mg−Por, while the oscillator strengths decrease gradually with each added water, so that a 10-fold reduction of the oscillator strength is observed between the uncomplexated Mg−Por and the Mg−Por with two waters. Such shifts and decreased peak heights can be observable in the experiment.[31] Interestingly, the states presented in Table 6 have a significant (10%) admixture of doubly excited configurations.

Table 6. Excitation Energies (in eV) and Oscillator Strengths for the Lowest Optical Allowed States of Mg−Por with n Water Ligands (n = 0, 1, 2)

n	excitation energy	oscillator strength
0	2.380	0.003
1	2.358	0.0011
	2.363	0.0014
2	2.331	0.0002
	2.348	0.0004

4. SUMMARY

Symmetry-adapted perturbation theory with monomers described on the DFT level has been utilized to calculate accurate interaction energies for complexes of magnesium−porphyrin with several ligands. The ZPVE and temperature effects were estimated on the DFT level. It has been found that all complexes of one ligand with Mg−Por are stable under standard conditions, while many complexes with two ligands are unstable due to large entropic effects. One-ligand complexes are always characterized by a bent Mg−Por, which results in a nonzero dipole moment of this molecule and therefore larger stabilization effects caused by the electrostatic and induction Mg−Por → ligand contributions. For the case of stable trimers, the dispersion energy is large enough to compensate for the reduction of the attraction caused by the planarization of Mg−Por in the trimer. We have found that trimers with pyridine, DMSO, imidazole, acetonitrile, and ethyl acetate are stable under standard conditions, although the stabilization of the last two is quite small. The complex with two water molecules has a free Gibbs energy close to zero at room temperature, and the available methods are not able to predict authoritatively its stability or instability. However, it can be safely assumed that this complex can be formed at temperatures slightly lower than 298.15 K. In the gas phase, the visible spectrum of the water complex of Mg−Por is predicted to be reduced in intensity and slightly red-shifted in comparison to the pure Mg−Por. We also show that popular MP2 and SCS-MP2 supermolecular energies are too low in the present case, which for the MP2 method leads to a wrong prediction of a stable complex of Mg−Por with two anionic ligands at 0 K. The behavior of SCS-MP2 is unfortunately also far from desired, as it gives interaction energies that are 5 to 10 mhartrees (3 to 6 kcal/mol) too low in comparison to the SAPT(DFT) results.

■ ASSOCIATED CONTENT

Supporting Information

Scan of the potential energy surface for Mg−Por−(acetylacetone (2))$_2$ trimer formation and geometry structures of the investigated dimers and trimers. This material is available free of charge via the Internet at http://pubs.acs.org.

■ AUTHOR INFORMATION

Corresponding Author

*E-mail: nczbik@cyf-kr.edu.pl; tania@chem.uw.edu.pl.

Notes

The authors declare no competing financial interest.

■ ACKNOWLEDGMENTS

T.K. acknowledges the support from the National Science Centre of Poland through grant 2011/01/B/ST4/06141.

■ REFERENCES

(1) Linnanto, J.; Korppi-Tommola, J. *Phys. Chem. Chem. Phys.* **2006**, *8*, 663.
(2) He, Z.; Sundström, V.; Pullerits, T. *J. Phys. Chem. B* **2002**, *106*, 11606.
(3) Orzeł, Ł.; Fiedor, L.; Wolak, M.; Kania, A.; van Eldik, R.; Stochel, G. *Chem.—Eur. J.* **2008**, *14*, 9419.
(4) Orzeł, Ł.; Kania, A.; Rutkowska-Zbik, D.; Susz, A.; Stochel, G.; Fiedor, L. *Inorg. Chem.* **2010**, *49*, 7362.
(5) Oba, T.; Tamiaki, H. *Photosynth. Res.* **2002**, *74*, 1.
(6) Balaban, T. S.; Fromme, P.; Holzwarth, A. R.; Krauß, N.; Prokhorenko, V. I. *Biochim. Biophys. Acta, Bioenerg.* **2002**, *1556*, 197.
(7) Bonnett, R.; Hursthouse, M. B.; Malik, K. M. A.; Mateen, B. *J. Chem. Soc., Perkin Trans. 2* **1977**, 2072.
(8) Ghosh, A.; Mobin, S. M.; Frölich, R.; Butcher, R. J.; Maity, D. K.; Ravikanth, M. *Inorg. Chem.* **2010**, *49*, 8287.
(9) Choon, O. C.; Rodley, G. *Inorg. Chim. Acta* **1983**, *79*, 166.
(10) Choon, O. C.; Rodley, G. *Inorg. Chim. Acta* **1983**, *80*, 177.
(11) Timkovich, R.; Tulinsky, A. *J. Am. Chem. Soc.* **1969**, *91*, 4430.
(12) Ong, C. C.; McKee, V.; Rodley, G. *Inorg. Chim. Acta* **1986**, *123*, L11.
(13) Fiedor, L. *Biochemistry* **2006**, *45*, 1910.
(14) Linnanto, J.; Korppi-Tommola, J. *Phys. Chem. Chem. Phys.* **2000**, *2*, 4962.
(15) Saitow, M.; Mochizuki, Y. *Chem. Phys. Lett.* **2012**, *525*, 144.
(16) Jarzęcki, A. A.; Kozlowski, P. M.; Pulay, P.; Ye, B.-H.; Li, X.-Y. *Spectrochim. Acta, Part A* **1997**, *53*, 1195.
(17) Lanzo, I.; Russo, N.; Sicilia, E. *J. Phys. Chem. B* **2008**, *112*, 4123.
(18) Sundholm, D. *Chem. Phys. Lett.* **1999**, *302*, 480.
(19) Sundholm, D. *Chem. Phys. Lett.* **2000**, *317*, 545.
(20) Ellervee, A.; Linnanto, J.; Freiberg, A. *Chem. Phys. Lett.* **2004**, *394*, 80.
(21) Elkin, M.; Ziganshina, O.; Berezin, K.; Nechaev, V. *J. Struct. Chem.* **2004**, *45*, 1086.
(22) Fredj, A. B.; Lakhdar, Z. B.; Ruiz-López, M. *Chem. Phys. Lett.* **2009**, *472*, 243.
(23) Grimme, S. *J. Comput. Chem.* **2004**, *25*, 1463.
(24) Grimme, S. *J. Comput. Chem.* **2006**, *27*, 1787.
(25) Grimme, S.; Antony, J.; Ehrlich, S.; Krieg, H. *J. Chem. Phys.* **2010**, *132*, 154104.
(26) Fredj, A. B.; Ruiz-López, M. F. *J. Phys. Chem. B* **2010**, *114*, 681.
(27) Heimdal, J.; Jensen, K.; Devarajan, A.; Ryde, U. *J. Biol. Inorg. Chem.* **2007**, *12*, 49.
(28) Rutkowska-Zbik, D.; Witko, M.; Fiedor, L. *J. Mol. Model.* DOI: 10.1007/s00894.012.1459.3.
(29) Dudev, T.; Lim, C. *Chem. Rev.* **2003**, *103*, 773.
(30) Kania, A.; Fiedor, L. *J. Am. Chem. Soc.* **2006**, *128*, 454.
(31) Fiedor, L.; Kania, A.; Myśliwa-Kurdziel, B.; Orzeł, Ł.; Stochel, G. *Biochim. Biophys. Acta, Bioenerg.* **2008**, *1777*, 1491.
(32) Grimme, S. *J. Chem. Phys.* **2003**, *118*, 9095.
(33) Hobza, P.; Selzle, H. L.; Schlag, H. W. *J. Phys. Chem.* **1996**, *100*, 18790.
(34) Korona, T.; Heßelmann, A.; Dodziuk, H. *J. Chem. Theory Comput.* **2009**, *5*, 1585.
(35) Jeziorski, B.; Moszynski, R.; Szalewicz, K. *Chem. Rev.* **1994**, *94*, 1887.
(36) Szalewicz, K.; Jeziorski, B. In *Molecular Interactions − from van der Waals to Strongly Bound Complexes*; Schreiner, S., Ed.; Wiley: New York, 1997; pp 3−43.
(37) Szalewicz, K.; Patkowski, K.; Jeziorski, B. *Struct. Bonding (Berlin)* **2005**, *116*, 43.
(38) Podeszwa, R.; Szalewicz, K. *Chem. Phys. Lett.* **2005**, *412*, 488.
(39) Heßelmann, A.; Jansen, G.; Schütz, M. *J. Chem. Phys.* **2005**, *122*, 014103.
(40) Korona, T.; Jeziorski, B. *J. Chem. Phys.* **2006**, *125*, 184109.
(41) Korona, T. *Phys. Chem. Chem. Phys.* **2007**, *9*, 6004.
(42) Korona, T.; Jeziorski, B. *J. Chem. Phys.* **2008**, *128*, 144107.
(43) Korona, T. *J. Chem. Phys.* **2008**, *122*, 224104.
(44) Korona, T. *Phys. Chem. Chem. Phys.* **2008**, *10*, 6509.
(45) Korona, T. *J. Chem. Theory Comput.* **2009**, *5*, 2663.
(46) Korona, T. In *Recent Progress in Coupled Cluster Methods*; Čársky, P., Paldus, J., Pittner, J., Eds.; Springer-Verlag: New York, 2010; p 267.
(47) Williams, H. L.; Chabalowski, C. F. *J. Phys. Chem. A* **2001**, *105*, 646.
(48) Misquitta, A. J.; Szalewicz, K. *Chem. Phys. Lett.* **2002**, *357*, 301.
(49) Misquitta, A. J.; Jeziorski, B.; Szalewicz, K. *Phys. Rev. Lett.* **2003**, *91*, 033201.
(50) Misquitta, A. J.; Podeszwa, R.; Jeziorski, B.; Szalewicz, K. *J. Chem. Phys.* **2005**, *123*, 214103.
(51) Jansen, G.; Heßelmann, A. *J. Phys. Chem. A* **2001**, *105*, 11156.
(52) Heßelmann, A.; Jansen, G. *Chem. Phys. Lett.* **2002**, *357*, 464.
(53) Heßelmann, A.; Jansen, G. *Chem. Phys. Lett.* **2002**, *362*, 319.
(54) Heßelmann, A.; Jansen, G. *Chem. Phys. Lett.* **2003**, *367*, 778.
(55) Heßelmann, A.; Jansen, G. *Phys. Chem. Chem. Phys.* **2003**, *5*, 5010.
(56) Dunlap, B. I.; Connolly, J. W. D.; Sabin, J. R. *J. Chem. Phys.* **1979**, *71*, 4993.
(57) Heßelmann, A.; Jansen, G.; Schütz, M. *J. Am. Chem. Soc.* **2006**, *128*, 11730.
(58) Podeszwa, R.; Bukowski, R.; Szalewicz, K. *J. Chem. Theory Comput.* **2006**, *2*, 400.
(59) Weigend, F. *Phys. Chem. Chem. Phys.* **2002**, *4*, 4285.
(60) Ahlrichs, R. *Phys. Chem. Chem. Phys.* **2004**, *6*, 5119.
(61) Podeszwa, R.; Bukowski, R.; Rice, B. M.; Szalewicz, K. *Phys. Chem. Chem. Phys.* **2007**, *9*, 5561.
(62) Korona, T.; Dodziuk, H. *J. Chem. Theory Comput.* **2011**, *7*, 1476.
(63) Jeziorska, M.; Jeziorski, B.; Cizek, J. *Int. J. Quantum Chem.* **1987**, *32*, 149.
(64) Moszynski, R.; Heijmen, T. G. A.; Jeziorski, B. *Mol. Phys.* **1996**, *88*, 741.
(65) Heßelmann, A.; Korona, T. *Phys. Chem. Chem. Phys.* **2011**, *13*, 732.
(66) Heßelmann, A. *J. Chem. Phys.* **2008**, *128*, 144112.
(67) Pitonak, M.; Heßelmann, A. *J. Chem. Theory Comput.* **2010**, *6*, 168.
(68) Chalasinski, G.; Szczesniak, M. M. *Mol. Phys.* **1988**, *63*, 205.
(69) Cybulski, S. M.; Chalasinski, G.; Moszynski, R. *J. Chem. Phys.* **1990**, *92*, 4357.
(70) Boys, S. F.; Bernardi, F. *Mol. Phys.* **1970**, *19*, 553.
(71) Dirac, P. A. M. *Proc. R. Soc. London, Ser. A* **1929**, *123*, 714.
(72) Slater, J. C. *Phys. Rev.* **1951**, *81*, 385.
(73) Vosko, S. H.; Wilk, L.; Nusair, M. *Can. J. Phys.* **1980**, *58*, 1200.
(74) Becke, A. D. *Phys. Rev. A* **1988**, *38*, 3098.
(75) Perdew, J. P. *Phys. Rev. B* **1986**, *33*, 8822.
(76) Ahlrichs, R.; Bär, M.; Häser, M.; Horn, H.; Kölmel, C. *Chem. Phys. Lett.* **1989**, *162*, 165.

(77) *TURBOMOLE V6.3 2011*; University of Karlsruhe and Forschungszentrum Karlsruhe GmbH: Karlsruhe, Germany, 1989–2007; TURBOMOLE GmbH: Karlsruhe, Germany, 2007. Available from http://www.turbomole.com (accessed October 2011).
(78) Eichkorn, K.; Treutler, O.; Öhm, H.; Häser, M.; Ahlrichs, R. *Chem. Phys. Lett.* **1995**, *240*, 283.
(79) Schafer, A.; Huber, C.; Ahlrichs, R. *J. Chem. Phys.* **1994**, *100*, 5829.
(80) Eichkorn, K.; Weigend, F.; Treutler, O.; Ahlrichs, R. *Theor. Chem. Acc.* **1997**, *97*, 119.
(81) Bassan, A.; Borowski, T.; Siegbahn, P. E. M. *Dalton Trans.* **2004**, 3153.
(82) Alecu, I. M.; Zheng, J.; Zhao, Y.; Truhlar, D. G. *J. Chem. Theory Comput.* **2010**, *6*, 2872.
(83) Hrenar, T.; Werner, H.-J.; Rauhut, G. *J. Chem. Phys.* **2007**, *126*, 134108.
(84) Werner, H.-J.; Knowles, P. J.; Manby, F. R.; Schütz, M.; Celani, P.; Knizia, G.; Korona, T.; Lindh, R.; Mitrushenkov, A.; Rauhut, G.; Adler, T. B.; Amos, R. D.; Bernhardsson, A.; Berning, A.; Cooper, D. L.; Deegan, M. J. O.; Dobbyn, A. J.; Eckert, F.; Goll, E.; Hampel, C.; Hesselmann, A.; Hetzer, G.; Hrenar, T.; Jansen, G.; Köppl, C.; Liu, Y.; Lloyd, A. W.; Mata, R. A.; May, A. J.; McNicholas, S. J.; Meyer, W.; Mura, M. E.; Nicklass, A.; Palmieri, P.; Pflüger, K.; Pitzer, R.; Reiher, M.; Shiozaki, T.; Stoll, H.; Stone, A. J.; Tarroni, R.; Thorsteinsson, T.; Wang, M.; Wolf, A. *MOLPRO*, version 2010.1; Cardiff University: Cardiff, U. K., 2010. See http://www.molpro.net (accessed October 2011).
(85) Perdew, J. P.; Burke, K.; Ernzerhof, M. *Phys. Rev. Lett.* **1996**, *77*, 3865.
(86) Adamo, C.; Barone, V. *J. Chem. Phys.* **1999**, *110*, 6158.
(87) Grüning, M.; Gritsenko, O. V.; van Gisergen, S. J. A.; Baerends, E. J. *J. Chem. Phys.* **2001**, *114*, 652.
(88) Computational Chemistry Comparison and Benchmark DataBase. http://cccbdb.nist.gov (accessed October 2011).
(89) Godbout, N.; Salahub, D. R.; Andzelm, J.; Wimmer, E. *Can. J. Chem.* **1992**, *70*, 560.
(90) Weigend, F.; Häser, M.; Patzelt, H.; Ahlrichs, R. *Chem. Phys. Lett.* **1998**, *294*, 143.
(91) Weigend, F.; Köhn, A.; Hättig, C. *J. Chem. Phys.* **2002**, *116*, 3175.
(92) Dudev, T.; Lim, C. *Acc. Chem. Res.* **2007**, *40*, 85.
(93) Helgaker, T.; Klopper, W.; Koch, H.; Noga, J. *J. Chem. Phys.* **1997**, *106*, 9639.
(94) Halkier, A.; Helgaker, T.; Jørgensen, P.; Klopper, W.; Koch, H.; Olsen, J.; Wilson, A. K. *Chem. Phys. Lett.* **1998**, *286*, 243.
(95) Halkier, A.; Helgaker, T.; Jørgensen, P.; Klopper, W.; Olsen, J. *Chem. Phys. Lett.* **1999**, *302*, 437.
(96) Anoop, A.; Thiel, W.; Neese, F. *J. Chem. Theory Comput.* **2010**, *6*, 3137.
(97) Neese, F.; Valeev, E. F. *J. Chem. Theory Comput.* **2011**, *7*, 33.
(98) Stanton, J. F.; Bartlett, R. J. *J. Chem. Phys.* **1993**, *98*, 7029.
(99) Korona, T.; Werner, H.-J. *J. Chem. Phys.* **2003**, *118*, 3006.
(100) Dunning, T. H., Jr. *J. Chem. Phys.* **1970**, *53*, 2823.